Asian Journal of Chemistry; Vol. 35, No. 12 (2023), 2979-2986

ASIAN JOURNAL OF CHEMISTRY

https://doi.org/10.14233/ajchem.2023.30319

Synthesis, Antimicrobial Activity and Dual Target Docking Studies of Novel 1-(5-Chloro-1-benzofuran-2-yl)-3-substituted Phenyl Prop-2-en-1-ones

BHARGAVI POSINASETTY[1,2], RAJENDRA PRASAD YEJJELLA[3], GEETHA BIRUDALA[4], KISHORE BANDARAPALLE[5], KOMARLA KUMARACHARI RAJASEKHAR[6,*] and NARESH BABU CHILAMAKURU[7]

[1]Department of Public Health, University of Southern Mississippi, MS-39406, USA
[2]Department of Dentistry, Government Dental College and Research Institute, Bellary-583104, India
[3]Department of Pharmaceutical Chemistry, University College of Pharmaceutical Sciences, Andhra University, Visakhapatnam-530003, India
[4]Faculty of Pharmacy, Dr. M.G.R. Educational and Research Institute, Velappanchavadi, Chennai-600077, India
[5]Department of Pharmaceutics, Sri Padmavathi School of Pharmacy, Tiruchanur, Tirupati-517503, India
[6]Department of Pharmaceutical Chemistry, Sri Padmavathi School of Pharmacy, Tiruchanur, Tirupati-517503, India
[7]Raghavendra Institute of Pharmaceutical Education and Research, Ananthapuramu-515721, India

*Corresponding author: Fax: +91 877 2237732; E-mail: komarla.research@gmail.com

Received: 20 September 2023; *Accepted*: 21 October 2023; *Published online*: 2 December 2023; AJC-21458

This study involved synthesizing five novel derivatives of 1-(5-chloro-1-benzofuran-2-yl)-3-substituted phenyl prop-2-en-1-ones through the Claisen-Schmidt condensation reaction, using 5-chloro-2-acetyl benzofuran and aromatic aldehydes in the presence of base catalyst. The chemical structures of these compounds were confirmed by using IR spectroscopy, ^{1}H NMR spectroscopy and mass spectrometry. Schrödinger docking simulations were employed to ascertain the binding affinity of the synthesized compounds to *Mycobacterium tuberculosis* enoyl-ACP reductase and *Escherichia coli* Topoisomerase IV. Subsequently, the anti-tubercular and *in vitro* antibacterial activities of the synthesized compounds were also investigated. Anti-tubercular efficacy was determined using the MABA method, while the antibacterial effectiveness was assessed against both Gram-positive and Gram-negative bacterial strains through the agar cup plate. The findings from these assays provide insights into the potential of these compounds as agents possessing anti-tubercular and antibacterial characteristics, thereby offering promising prospects for further investigation in the field of drug development.

Keywords: Benzofuranyl chalcones, Antibacterial activity, Anti-tubercular activity, Dual target docking.

INTRODUCTION

Co-infections and super-infections associated with severe acute respiratory syndrome coronavirus 2 (SARS-CoV-2) typically arise from either community-acquired bacteria or hospital acquired multidrug-resistant bacteria and fungi. Among these pathogens, *Mycobacterium tuberculosis* (MTB), the causative agent of tuberculosis, is capable of causing co-infection in coronavirus disease 2019 (COVID-19). The simultaneous presence of both COVID-19 and tuberculosis complicates the diagnosis and treatment of COVID-19, significantly increasing the risks of mortality and hindered recovery [1-4].

Reports from the World Health Organization (WHO) indicate that the COVID-19 pandemic has reversed years of progress in delivering essential MTB services and reducing the burden of MTB disease. Despite some achievements in specific regions, global MTB targets remain largely unmet, with a significant reduction in the number of newly diagnosed and reported MTB cases worldwide. Treating these co-infections with broad spectrum empiric antibiotics can increase the likelihood of developing multidrug resistance [5,6]. Furthermore, co-infections and super-infections, particularly in resource-limited regions, are believed to contribute to the relatively higher rates of severe infection and mortality associated with SARS-CoV-2. The presence of bacterial or fungal co-infections alongside SARS-CoV-2 is associated with a higher mortality rate. Although the occurrence of tuberculosis co-infection with COVID-19 is very low, it continues to be a matter of considerable concern, particularly among persons at high risk [7-9].

The chalcone class of enones, also known as 1,3-diaryl-2-propen-1-ones, has played a pivotal role in the fields of organic

and medicinal chemistry for over a century. Heterocyclic chalcones, a subset of synthetic chalcone derivatives, are particularly significant in medicinal chemistry due to the prevalence of heterocyclic scaffolds in biologically active compounds [10-14]. Research has unequivocally established that heteroaromatic hybrid chalcones possess significant medicinal value. They have demonstrated efficacy as anticancer, antimicrobial, antifungal, antituberculosis, antiparkinsonian, anti-inflammatory agents, while also serving essential pharmacological functions. Furthermore, these compounds have practical applications in agrochemistry, where they function as photosynthesis inhibitors and in the industrial sector, where they serve as photoinitiators in 3D printing processes [15-25].

In this work, the synthesis and assessment of antitubercular and antibacterial activity for novel five benzofuranylchalcones *viz.*1-(5-chloro-1-benzofuran-2-yl)-3-substituted phenyl prop-2-en-1-ones were carried out. These compounds were generated by introducing various substitutions at the B-ring position of chalcone. The synthesized compounds (**3a-e**) were also docked against two specific protein targets *e.g.* enoyl-acyl carrier protein reductase (InhA) in *M. tuberculosis* (MTB) and topoisomerase IV (Topo IV) in *E. coli*. The purpose of this dual-target docking analysis was to predict the binding affinity of the synthesized chalcone derivatives toward InhA and Topo IV. This prediction could be instrumental in identifying the potential correlations between binding affinity to these two targets and the minimum inhibitory concentration (MIC) for heteroarylchalcone-based antimicrobial drugs. Additionally, the dual-target docking results can provide valuable insights for subsequent investigations into the structure based drug design of heteroarylchalcone based antimicrobial drugs.

EXPERIMENTAL

All chemicals were procured from Sigma-Aldrich Co. (St. Louis, USA), Merck (Whitehouse Station, NJ, USA), Qualigens Fine Chemicals (Mumbai, India), Loba Chemie Pvt. Ltd (Mumbai, India) and Himedia Laboratories Pvt. Ltd (Mumbai, India). To determine the melting points of the synthesized compounds, we utilized a digital melting point apparatus with open capillary tubes and the provided values are uncorrected. Thin layer chromatography technique was used to assess the purity of the compounds. This involved pre-coated silica gel strips and a solvent system consisting of hexane:ethyl acetate (2:1). The spots were then detected using an ultraviolet chamber.

Characterization: Infrared spectra were recorded with a Shimadzu FT-IR 4000 instrument, using KBr disks. The CHNO elemental analysis was carried out using the Perkin-Elmer Series II 2400 CHNS/O elemental analyzer. Mass spectra were acquired using a JEOL GC mate II GC-Mass spectrometer at 70 eV, employing the direct insertion probe method. Nuclear magnetic resonance (NMR) spectra were acquired utilizing a Bruker AVIII-500 MHz FT-NMR spectrometer, with tetramethylsilane as the internal standard and DMSO as solvent.

Synthetic procedure: As shown in **Scheme-I**, the title compounds were synthesized starting from 5-chlorosalicylaldehyde (**1**). Initially, 5-chlorosalicylaldehyde (**1**) under-went cyclization to yield the subsequent crucial synthon, 5-chloro-2-acetylbenzofuran (**2**). Subsequently, the acetyl functionality was transformed into prop-2-en-1-one through Claisen-Schmidt condensation reaction with aromatic aldehydes. This series of chemical transformations led to the formation of the title compounds, namely, 1-(5-chloro-1-benzofuran-2-yl)-3-substituted phenyl prop-2-en-1-ones (**3a-e**).

Synthesis of 5-chloro-2-acetylbenzofuran (2): A mixture containing 5-chlorosalicylaldehyde (**1**), chloroacetone (4.63 g, 0.05 mol) and anhydrous potassium carbonate (15 g) was gently refluxed in dry acetone (50 mL) for a duration of 12 h. After the completion of the reaction, the reaction product was filtered and the filtrate was subjected to solvent removal under reduced pressure yielded 5-chloro-2-acetylbenzofuran (**2**) as a light brownish solid. The obtained product was further purified by recrystallization from ethanol, resulting in a yield of 75% having m.p. 83-85 ºC. IR (KBr, ν_{max}, cm^{-1}): 1666 (C=O), 1461 (C=C) and 790 (CCl), MS (*m/z*, %): 194 (M^+) and 196 ($M+2^+$), ^{1}H NMR (δ ppm): 7.2-7.8 (4Ar-H), 2.6 (3H, s, CH_3).

General synthesis of 1-(5-chloro-1-benzofuran-2-yl)-3-(substitutedphenyl)-prop-2-en-1-ones (3a-e): A mixture consisting of 5-chloro-2-acetylbenzofuran (**2**) (1.94 g, 0.01 mol) and various substituted aromatic aldehydes (0.01 mol), in 50 mL of ethanol was cooled to 5-10 ºC. Aqueous sodium hydroxide (70%, 5 mL) was then added dropwise with constant stirring. The reaction mixture was further stirred for a duration of 2 h and left overnight. Subsequently, it was neutralized with conc. HCl. The solid product that separated out was collected and it was further purified by crystallization from ethanol. The purity of all synthesized compounds was confirmed by thin-layer chromatography (TLC) using a mobile phase consisting of a mixture of *n*-hexane and ethyl acetate.

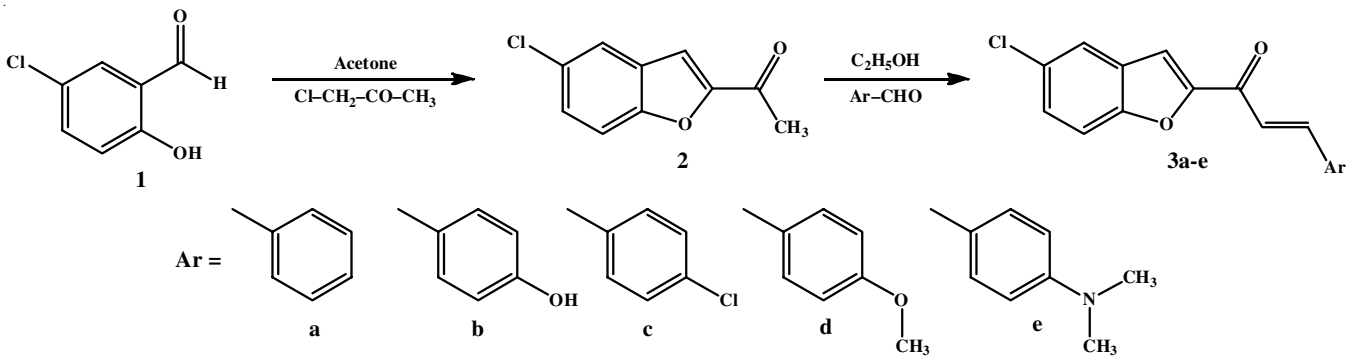

Scheme-I: General synthesis of 1-(5-chloro-1-benzofuran-2-yl)-3-substituted phenyl prop-2-en-1-ones (**3a-e**)

1-(5-Chloro-1-benzofuran-2-yl)-3-phenylprop-2-en-1-one (3a): Yield: 75%: m.p.: 110-114 ºC; FT-IR (KBr, ν_{max}, cm^{-1}): 1650 (C=O), 1438 (C=C), 800 (C-Cl); ^{1}H NMR (DMSO-d_6, δ ppm): 6.70 (1H, d), 7.26-7.56 (6H, 7.32 (dd), 7.41 (dd), 7.48 (tt), 7.49 (dd), 7.61-7.80 (3H, 7.63 (dd), 7.72 (dd), 7.74 (dd), 7.98 (1H, dd); MS (*m/z*, %): 282.12 (M^+). Anal. calcd. (found) % for $C_{17}H_{11}O_2Cl$: C, 72.33 (72.34); H, 3.88 (3.91); Cl, 12.54 (12.62); O, 11.32 (11.38).

1-(5-Chloro-1-benzofuran-2-yl)-3-(4-hydroxyphenyl)-prop-2-en-1-one (3b): Yield: 62%: m.p.: 148-153 ºC; FT-IR (KBr, ν_{max}, cm^{-1}): 3747 (OH), 1662 (C=O), 1442 (C=C), 805 (C-Cl); ^{1}H NMR (DMSO-d_6, δ ppm): 6.65 (1H, d), 6.89 (2H, dd), 7.31 (1H, dd), 7.47-7.62 (3H, 7.54 (d), 7.55 (dd), 7.65-7.89 (3H, 7.71 (dd), 7.73 (dd), 7.84 (dd), 9.8 (1H,s); MS (*m/z*, %): 298.12 (M^+), 300.04 $(M+2)^+$. Anal. calcd. (found) % for $C_{17}H_{11}O_3Cl$: C, 68.47 (68.45); H, 3.71 (3.69); Cl, 11.87 (11.92); O, 16.02 (16.08).

1-(5-Chloro-1-benzofuran-2-yl)-3-(4-chlorophenyl)-prop-2-en-1-one (3c): Yield: 70%: m.p.: 170-172 ºC; FT-IR (KBr, ν_{max}, cm^{-1}): 1650 (C=O), 1448 (C=C), 780 (C-Cl); ^{1}H NMR (DMSO-d_6, δ ppm): 6.75 (1H, d), 7.31 (1H, dd), 7.47-7.80 (7H, 7.53 (dd), 7.55 (dd), 7.61 (dd), 7.71 (dd), 7.74 (dd), 7.97 (1H, dd); MS (*m/z*, %): 317.23 (M^+). Anal. calcd. (found) % for $C_{17}H_{10}O_2Cl_2$: C, 64.56 (64.61); H, 3.18 (3.21); Cl, 22.34 (22.38); O, 10.11 (10.18).

1-(5-Chloro-1-benzofuran-2-yl)-3-(4-methoxyphenyl)-prop-2-en-1-one (3d): Yield: 88%: m.p.: 124-127 ºC; FT-IR (KBr, ν_{max}, cm^{-1}): 1668 (C=O), 1459 (C=C), 804 (C-Cl); ^{1}H NMR (DMSO-d_6, δ ppm): 3.83 (3H, s), 6.64 (1H, d), 7.13-7.37 (3H, 7.19 (dd), 7.31 (dd), 7.42-7.61 (3H, 7.48 (dd), 7.54 (d), 7.65-7.89 (3H, 7.71 (dd), 7.73 (dd), 7.84 (dd); MS (*m/z*, %): 312.28 (M^+). Anal. calcd. (found) % for $C_{18}H_{13}O_3Cl$: C, 69.15 (69.19); H, 4.20 (4.25); Cl, 11.34 (11.38); O, 15.37 (15.42).

1-(5-Chloro-1-benzofuran-2-yl)-3-[4-(dimethylamino) phenyl]prop-2-en-1-one (3e): Yield, 65%: m.p.: 135-138 ºC; FT-IR (KBr, ν_{max}, cm^{-1}): 1630 (C=O), 1456 (C=C) 814 (C-Cl); ^{1}H NMR (DMSO-d_6, δ ppm): 3.83 (3H, s), 6.64 (1H, d), 7.13-7.37 (3H, 7.19 (dd), 7.31 (dd), 7.42-7.61 (3H, 7.48 (dd), 7.54 (dd), 7.65-7.89 (3H, 7.71 (dd), 7.73 (dd), 7.84 (dd); MS (*m/z*, %): 325.11 (M^+). Anal. calcd. (found) % for $C_{19}H_{16}NO_2Cl$: C, 70.05 (70.11); H, 4.98 (4.93); Cl, 10.84 (12.89): N, 4.30(4.36); O, 9.81 (9.87).

Dual target docking studies

Preparation of target molecules: For the preparation of target molecules, the dual target docking study utilized the GLIDE docking program (Schrödinger 2020-1) [26]. The synthesized compounds (**3a-e**) were subjected to docking within the active sites of two crystal structures *e.g*. *Mycobacterium tuberculosis* enoyl-ACP reductase (PDB code: 2PR2) and *Escherichia coli* Topoisomerase IV ParE 24kDa subunit (PDB code: 1S14). The quality of the target protein structures underwent thorough assessment using various tools, including ERRAT, verify 3D and the structural analysis and verification server [27-29]. These analyses confirmed the acceptability and high quality of all protein models. Additionally, a comprehensive Ramachandran plot analysis was performed *via* RAMPAGE to evaluate dihedral angles and permissible conformations [30].

Preparation of ligand molecules: In the preparation of ligand molecules, the 2D chemical structures of compounds **3a-e** were drawn using Chem Draw Ultra Version 8.0.3 [31] and saved in binary format. These structures were subsequently converted into the SDF format using the Open Babel GUI version 2.4.1, a versatile virtual screening tool designed for Windows [32,33].

Following this, meticulous energy minimization was carried out using the OPLS3e force field with Ligprep. Key considerations included factors such as ionization at a target pH of 7.0 ± 2.0, desalting and the preservation of specified chiralities [34]. To facilitate a comparative assessment of binding affinities, ATP served as the reference ligand in the docking experiments and the results were comprehensively evaluated by scrutinizing binding interactions and docking scores derived from GLIDE_SP ligand docking.

Anti-tubercular activity: The synthesized derivatives, namely, 1-(5-chloro-1-benzofuran-2-yl)-3-substituted phenyl prop-2-en-1-ones (**3a-e**), underwent screening for antitubercular activity using the microplate Alamar blue assay method (MABA). Each of the synthesized compounds was assessed against the *M. tuberculosis* H37 RV strain, with isonicotinic acid hydrazide (INH) serving as standard drug for comparison.

To set up the assay, 200 µL of sterile deionized water was added to the outer perimeter wells of a sterile 96-well plate to minimize medium evaporation during incubation. Subsequently, 100 µL of Middlebrook 7H9 (MB 7H9) broth was dispensed into the wells and the synthesized compounds were serially diluted directly on the plate. The antitubercular activity of these compounds was assessed at final drug concentrations of 0.2, 0.4, 0.8, 1.6, 3.125, 6.25, 12.5, 25, 50 and 100 µg/mL. The plates were covered and sealed with parafilm, then incubated at 37 ºC for 5 days. After this incubation period, 25 µL of freshly prepared 1:1 mixture of Alamar blue reagent and 10% Tween-80 was added to each well. The plates were then incubated for an additional 24 h. A blue color indicated no bacterial growth, while a pink color was indicative of bacterial growth [35]. The minimum inhibitory concentration (MIC) was determined as the lowest drug concentration that prevented the colour change from blue to pink. Specifically, the MIC was defined as the concentration required to inhibit 90% of the standardized bacterial inoculum.

Antibacterial activity: The antibacterial activity of the synthesized compounds (**3a-e**) was assessed using the agar cup plate method. Specifically, these compounds were tested against both Gram-negative organisms, namely *Escherichia coli* and *Pseudomonas aeruginosa* and Gram-positive organisms, including *Staphylococcus epidermatitis* and *Bacillus subtilis*. The minimum inhibitory concentration (MIC) method was employed for the evaluation, with ciprofloxacin serving as a reference standard for result comparison.

For the procedure, brain heart infusion agar was maintained at room temperature. Colonies were transferred to the plates and their turbidity was visually adjusted using broth to match the turbidity of a 0.5 McFarland turbidity standard that had been vortexed. To ensure an even distribution, the entire surface of agar plate was swabbed three times, with the plates

rotated approximately 60º between streaking. Following this, the inoculated plate was allowed to stand for at least 5 min before the application of drugs. A 5 mm hollow tube was heated and pressed onto the inoculated agar plate, developing five wells in the plate, which were then promptly removed. Subsequently, 75, 50, 25, 10 and 5 µL of the synthesized compounds were added into the respective wells on each plate. The plates were then incubated within 15 min and then kept in an incubator at 37 ºC for 24 h. The MIC procedure involved repeating the serial dilution up to a 10^{-9} dilution for each synthesized compound [36,37].

RESULTS AND DISCUSSION

Traditionally, chalcones can be synthesized *via* the Claisen-Schmidt reaction, involving the reflux of a ketone and aldehyde in an organic solvent, often in the presence of an acid or base catalyst. In this study, the essential intermediate, 5-chloro-2-acetyl benzofuran (**2**) was synthesized by condensing 5-chloro-salicylaldehyde (**1**) with chloroacetone. This pivotal intermediate **2** was then subjected to the Claisen-Schmidt reaction with various aryl aldehydes to obtain the title compounds (**3a-e**).

The purity of all the synthesized compounds (**2** and **3a-e**) was confirmed using thin-layer chromatography (TLC), employing a hexane and ethyl acetate mixture as mobile phase. Their identity was further verified by exhibiting a single spot on TLC, sharp melting points and characteristic spectral features.

In the infrared (IR) spectra of the synthesized compounds (**2** and **3a-e**), a distinct band in the range between 1630 and 1666 cm^{-1} was observed, confirming the presence of an α,β-unsaturated ketone system. In ^1H NMR spectra of these compounds, signals for aromatic protons resonated within the range of 7.2 to 7.9 ppm, while signals for =CH-CO- were observed around 6.6 ppm. Notably, compound **3b** exhibited a proton singlet at 9.8 ppm, corresponding to the proton of hydroxy group located at the *para*-position of phenyl ring attached to the α,β-unsaturated ketone system. Mass spectra analysis further confirmed the presence of the expected molecular ion peak (M^+) fragments for the synthesized compounds. Remarkably, compound **3b** displayed two distinctive peaks at 298 $(M)^+$ and 300 $(M+2)^+$ *m/z*.

Antimicrobial activity: The synthesized benzofuranyl-chalcones (**3a-e**) were subjected to test against *M. tuberculosis* H37Rv in Middlebrook 7H9 broth media (MB 7H9 broth), with isoniazid (INH) employed as standard drug (Table-1). The results of the antitubercular activity screening indicated that compound **3e**, featuring *p*-dimethylamino, compound **3a**, which possesses an unsubstituted phenyl ring and compound **3d**, featuring *p*-methoxy on the aromatic moiety at the B-ring position of chalcone, exhibited activity at concentrations of 50 and 100 µg/mL. However, the remaining two compounds, **3b** and **3c**, did not demonstrate a significant activity in this context. Furthermore, all the synthesized compounds underwent evaluation for their antibacterial activity using the agar cup-plate method, with ciprofloxacin serving as the reference standard. Among these compounds (**3a-e**), notable antibacterial activity was observed at a dose level of 100 µg, compared to the standard drug (Fig. 1).

TABLE-1
ANTITUBERCULAR ACTIVITY OF SYNTHESIZED COMPOUNDS (**3a-e**)

Compound code	Minimum inhibitory concentration		
	25 µg/mL	50 µg/mL	100 µg/mL
Isoniazid	Sensitive	Sensitive	Sensitive
3a	Resistant	Resistant	Sensitive
3b	Resistant	Resistant	Resistant
3c	Resistant	Resistant	Resistant
3d	Resistant	Resistant	Sensitive
3e	Resistant	Sensitive	Sensitive

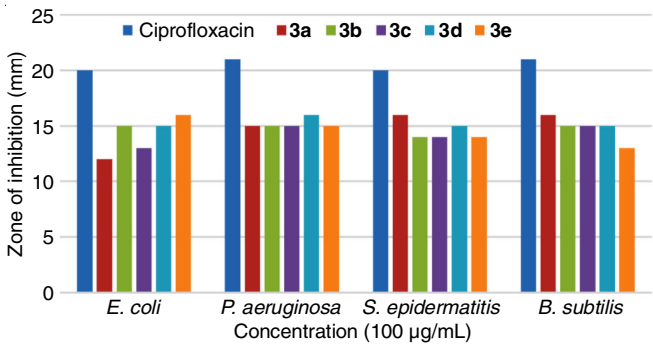

Fig. 1. Antibacterial activity of synthesized compounds **3a-e**

In particular, compound **3a** exhibited the highest activity against Gram-negative bacterial strains, likely due to the presence of an unsubstituted phenyl ring at the B-ring position of the chalcone. Additionally, all the compounds displayed substantial antibacterial activity against various bacterial strains, which can be attributed to the presence of various substituents at the *para*-position of the aryl rings, including chloro, hydroxyl, dimethylamino and methoxy groups, in addition to the favourable impact of 5-chlorobenzofuran moiety.

Dual target docking studies: The quality of the 3D target molecule models was assessed using Ramachandran plot calculations with RAMPAGE. The percentage of residues in the favoured region, allowed region and outlier region was determined to be 89.8%, 8.9% and 0.9% for 2PR2 and 94.6%, 5.4% and 0% for 1S14, respectively. Typically, a score close to 100% indicates good model quality, suggesting that the predicted models were of good quality (Fig. 2).

Additionally, these structures were validated by other servers such as ERRAT and Verify 3D. The overall quality factor of the target molecules, as obtained in ERRAT analysis, followed the order of 94.21% (2PR2) < 95.83% (1S14). All these values are either higher or very close to the 95% rejection limit, further confirming the quality of the target protein models. In verify 3D analysis, it was observed that none of the amino acids of 2PR2 had a negative score, but a few residues in 1S14 exhibited marginal negative scores. The percentage of amino acid residues with a 3D-1D score greater than or equal to 0.2 was 99.25% for 2PR2 and 46.43% for 1S14. It is important to observe that compatibility scores above zero indicate an acceptable structural environment (Fig. 3).

The docking scores for each ligand against both target proteins were predicted using Glide, a widely utilized docking software developed by Schrödinger. Figs. 4 and 5 show the docking of compounds **3a-e** with the two target protein models.

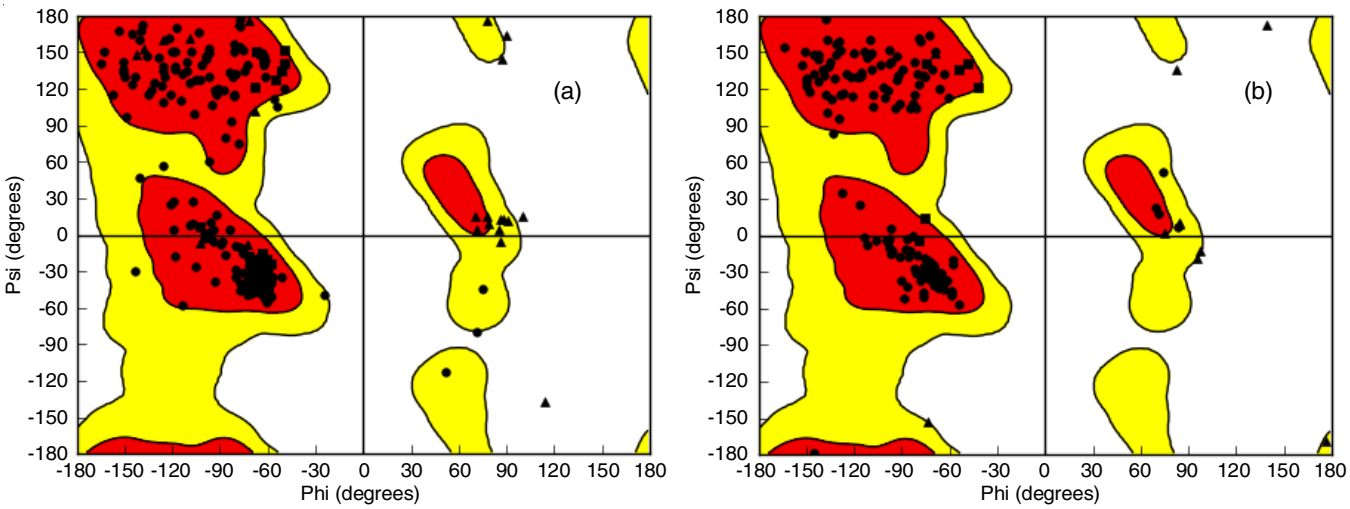

Fig. 2. Ramachandran plots generated *via* RAMPAGE for (a) 2PR2 and (b) 1S14. Residues in favoured (red), allowed (yellow) and outlier regions (white)

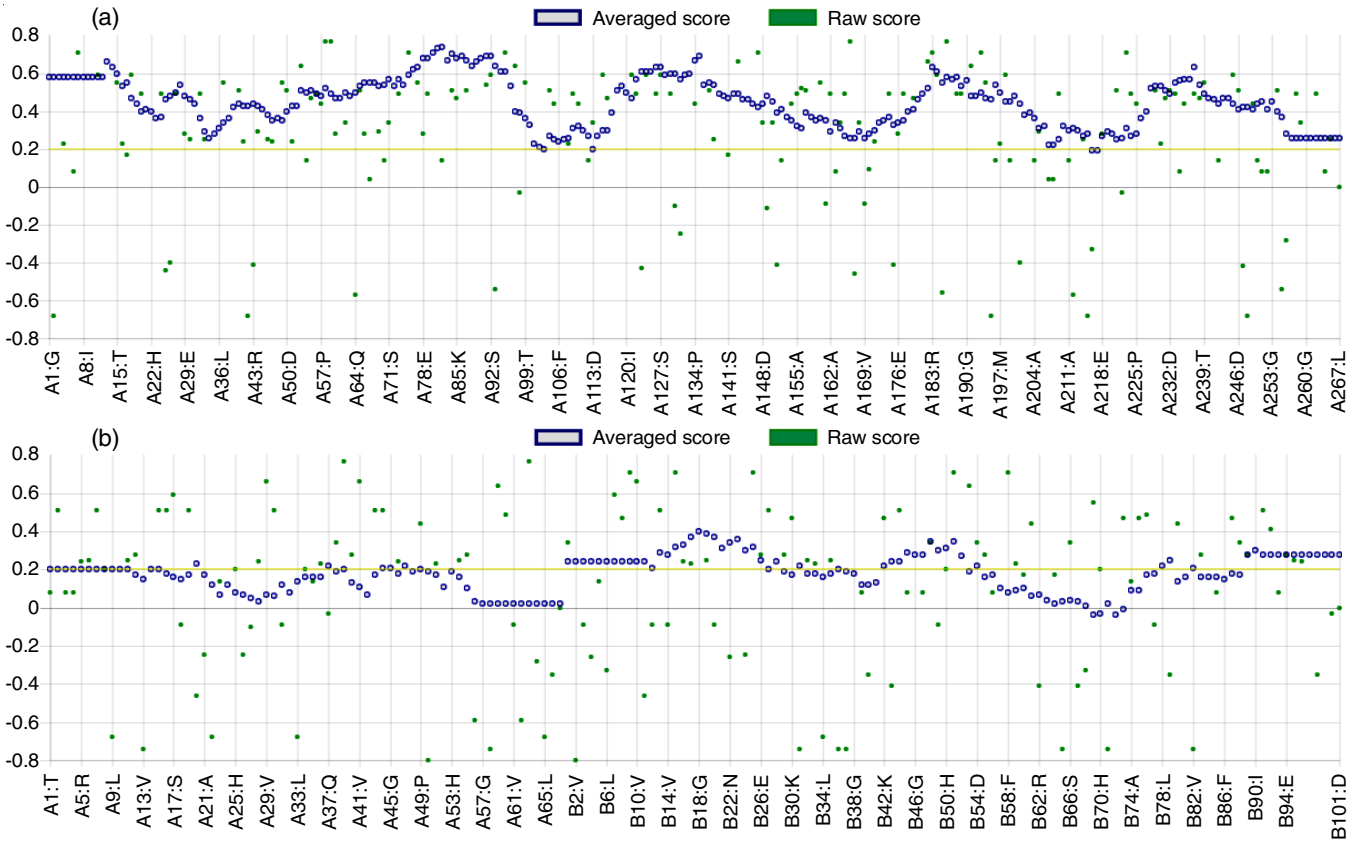

Fig. 3. Verify 3D results of (a) 2PR2 and (b) 1S14

In docking process, ten binding poses were obtained and the binding pose with the highest docking score was selected. Among all the synthesized compounds, compound **3b** exhibited the highest docking score (-5.66 1S14). All the compounds displayed interesting docking scores comparable to their respective standards.

A summary of the interactions observed between the synthesized compounds (**3a-e**) and amino acid residues of the target proteins 2PR2 and 1S14 is presented in Tables 2 and 3. With the exception of compounds **3d** and **3e**, all the synthesized compounds displayed hydrophobic interactions with 2PR2. Except for **3a**, **3d** and **3e**, compounds **3b** and **3c** exhibited hydrophobic interactions similar to the standard drug isoniazid. Conversely, compounds **3d** and **3e** did not demonstrate any hydrophobic interactions with the target 2PR2.

Furthermore, all the synthesized compounds, except compound **3c**, engaged in hydrogen bond interactions, *albeit* at different binding sites. Compounds **3a** and **3b** were unique in that they interacted with both hydrophobic pockets and hydrogen binding residues, while the remaining compounds interacted

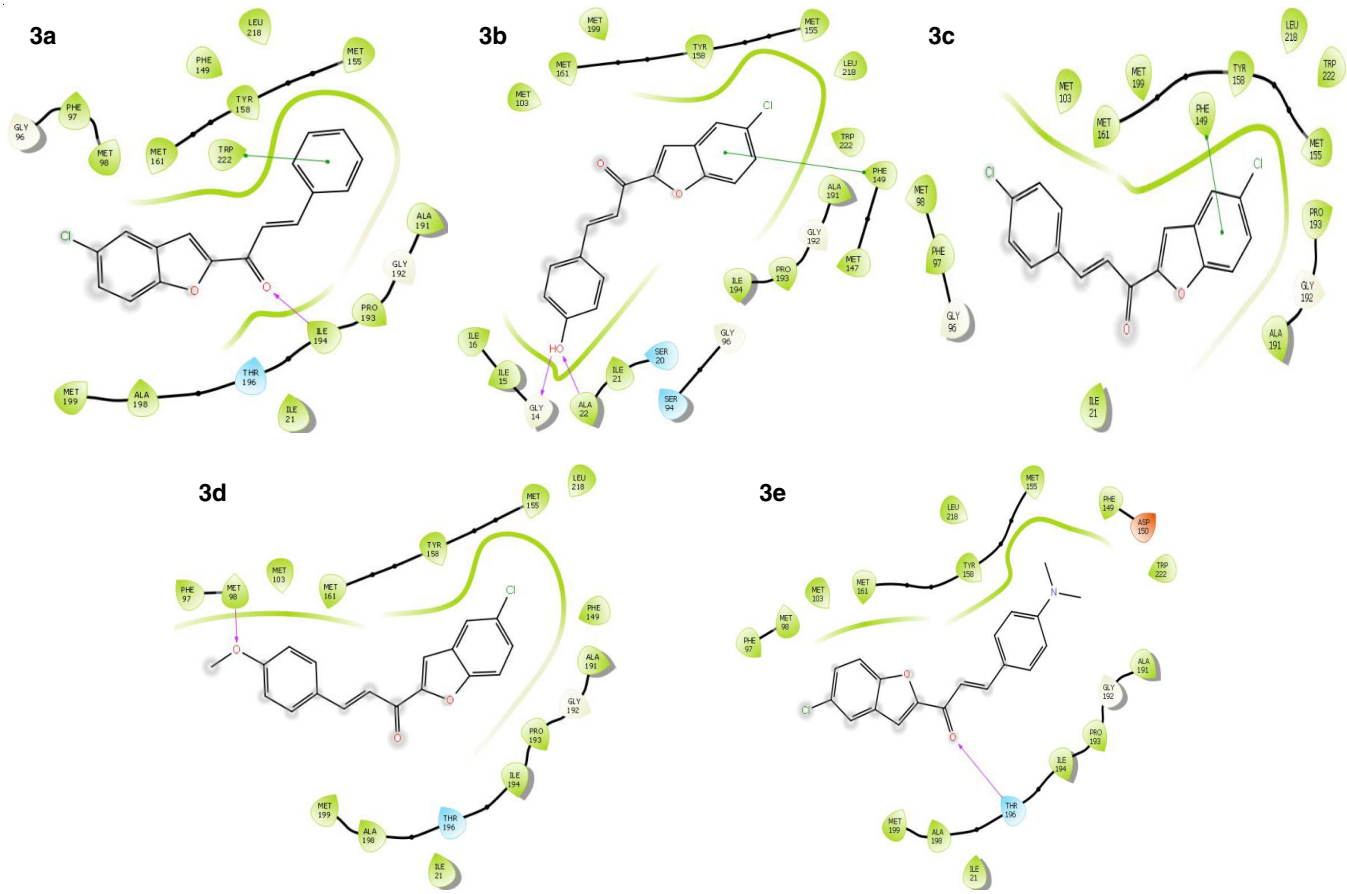

Fig. 4. Docking of synthesized compounds **3a-e** with 2PR2 protein

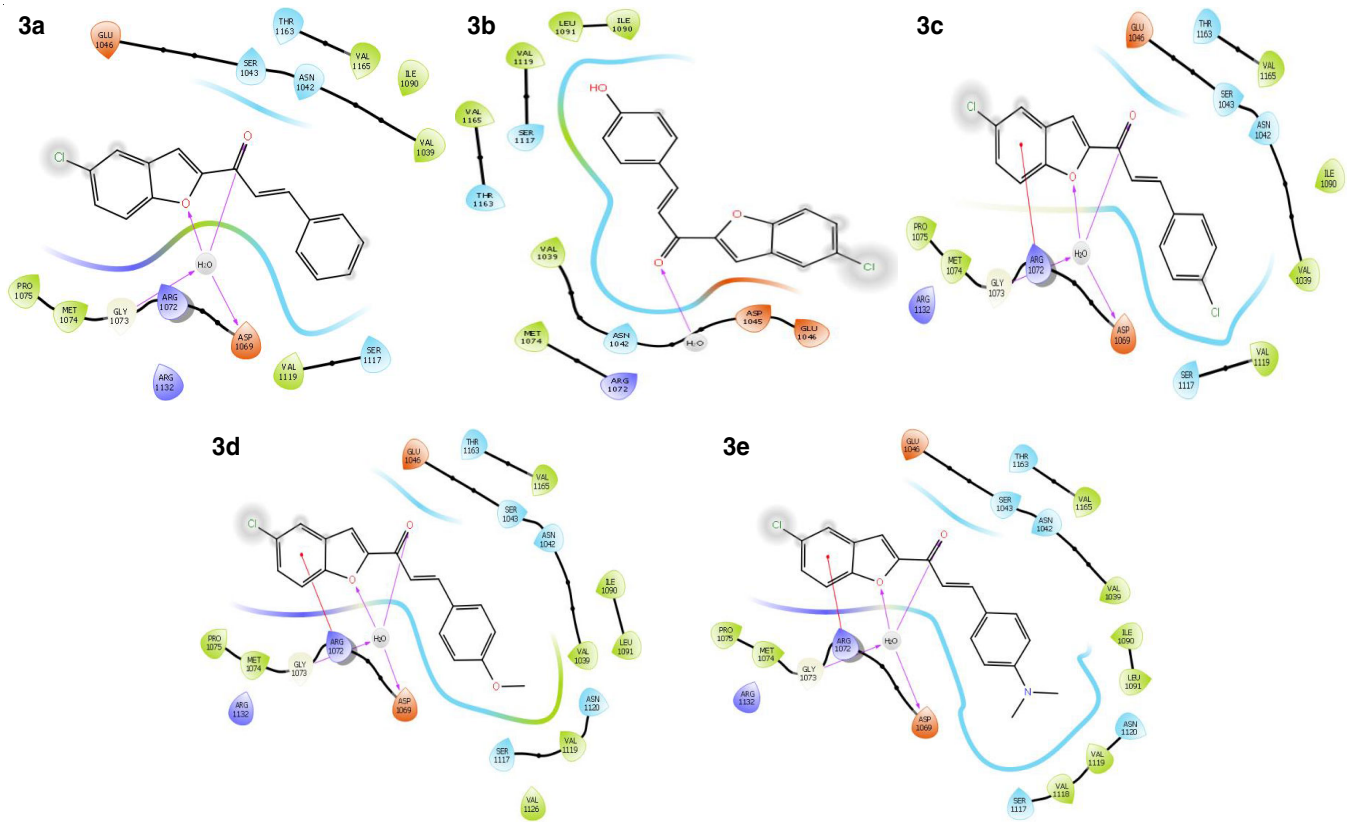

Fig. 5. Docking of synthesized compounds **3a-e** with 1S14 protein

TABLE-2
DOCKING SCORE AND MOLECULAR INTERACTION OF SYNTHESIZED COMPOUNDS WITH 2PR2 PROTEIN

Compound code	Docking score	H-Bond interactions	Hydrophobic interactions (Pi-Pi stacking or Pi-cation)
3a	-7.980	ILE 194	TRP 222
3b	-8.151	GLY 14, ALA 22	PHE 149
3c	-7.664	–	PHE 149
3d	-7.705	MET 98	–
3e	-7.797	THR 196	–
Isoniazid	-7.244	VAL 95, GLY 96	PHE 41

TABLE-3
DOCKING SCORE AND MOLECULAR INTERACTION OF SYNTHESIZED COMPOUNDS WITH 1S14 PROTEIN

Compound code	Docking score	H-Bond interactions	Hydrophobic interactions
3a	-6.47	ASP 1069, GLY 1073	–
3b	-5.66	–	–
3c	-6.596	ASP 1069, GLY 1073	ARG 1072
3d	-6.792	ASP 1069, GLY 1073	ARG 1072
3e	-6.936	ASP 1069, GLY 1073	ARG 1072
Ciprofloxacin	-7.066	ASP 1069, GLY 1073	VAL 1118

with either hydrophobic pockets or hydrogen bonding residues. All the synthesized compounds achieved docking scores that were close to the standard's score, indicating nearly equivalent binding affinity. It is indeed interesting to observe that all the synthesized compounds, except for compound **3b**, shared the same hydrogen bond interaction sites in the 1S14 protein model, which were comparable to the standard. However, they differed from the standard in terms of hydrophobic interaction sites. Specifically, synthesized compounds **3c**, **3d** and **3e** exhibited hydrophobic interactions at the same site. Notably, compound **3c** did not show either hydrogen bond or hydrophobic interactions, yet it surprisingly achieved the highest docking score.

Conclusion

In this study, the critical issue of co-infections and super-infections associated with SARS-CoV-2, highlighting their impact on diagnosis, treatment and the global burden of tuberculosis. Thus, the synthesis and characterization of novel compounds, 1-(5-chloro-1-benzofuran-2-yl)-3-substituted phenyl prop-2-en-1-ones (**3a-e**) with the aim of exploring their potential as antimicrobial agents were carried out. The *in vitro* anti-tubercular and antibacterial activities revealing the promising results. The synthesized compounds with electron-donating groups on the aromatic ring exhibited strong antimicrobial activity. In addition to experimental assays, the dual-target docking studies were also conducted to predict the binding affinity of the compounds (**3a-e**) to *Mycobacterium tuberculosis* enoyl-ACP reductase and *Escherichia coli* Topoisomerase IV. These computational analyses provided insights into their potential as lead structures for future drug design.

ACKNOWLEDGEMENTS

The authors are thankful for the research support received from Sri Padmavathi School of Pharmacy, Tirupati and Raghavendra Institute of Pharmaceutical Education and Research, Ananthapuramu, India.

CONFLICT OF INTEREST

The authors declare that there is no conflict of interests regarding the publication of this article.

REFERENCES

1. F. Bantun, *J. Fungi*, **9**, 598 (2023); https://doi.org/10.3390/jof9060598
2. M. Shafiekhani, Z. Shekari, A. Boorboor, Z. Zare, S. Arabsheybani and N. Azadeh, *Virol. J.*, **19**, 35 (2022); https://doi.org/10.1186/s12985-022-01763-9
3. A.M. Alnimr, M.S. Alshahrani, S. Alwarthan, S.Y. AlQahtani, A.A. Hassan, N.N. BuMurah, S. Alhajiri and H. Bukharie, *J. Epidemiol. Glob. Health*, **12**, 188 (2022); https://doi.org/10.1007/s44197-022-00038-4
4. M.S. Gerver, R. Guy, K. Wilson, S. Thelwall, O. Nsonwu, G. Rooney, C.S. Brown, B. Muller-Pebody, R. Hope and V. Hall, *Clin. Microbiol. Infect.*, **27**, 1658 (2021); https://doi.org/10.1016/j.cmi.2021.05.040
5. P. Daneshvar, B. Hajikhani, F. Sameni, N. Noorisepehr, F. Zare, N. Bostanshirin, S. Yazdani, M. Goudarzi, S. Sayyari and M. Dadashi, *Heliyon*, **9**, e13637 (2023); https://doi.org/10.1016/j.heliyon.2023.e13637
6. E. Luke, K. Swafford, G. Shirazi and V. Venketaraman, *Front. Biosci. (Schol. Ed.)*, **14**, 6 (2022); https://doi.org/10.31083/j.fbs1401006
7. T. Shah, Z. Shah, N. Yasmeen, Z. Baloch and X. Xia, *Front. Immunol.*, **13**, 909011 (2022); https://doi.org/10.3389/fimmu.2022.909011
8. *Eur. Respir. J.*, **59**, 2102538 (2022); https://doi.org/10.1183/13993003.02538-2021
9. H. Mollalign, D. Chala and D. Beyene, *Infect. Drug Resist.*, **15**, 4037 (2022); https://doi.org/10.2147/IDR.S370837
10. A. Mallia and J. Sloop, *Molecules*, **28**, 3201 (2023); https://doi.org/10.3390/molecules28073201.
11. A. Urbonavicius, G. Fortunato, E. Ambrazaityte, E. Plytninkiene, A. Bieliauskas, V. Milišiunaite, R. Luisi, E. Arbaciauskiene, S. Krikštolaityte and A. Šackus, *Molecules*, **27**, 3752 (2022); https://doi.org/10.3390/molecules27123752
12. M. El-Naggar, H.R.M. Rashdan and A.H. Abdelmonsef, *ACS Omega*, **8**, 27216 (2023); https://doi.org/10.1021/acsomega.3c02478
13. M. Ali Hazam, R.J. Mahesein and H.N.K.AL-Salman, *J. Population Therapeutics and Clinical Pharmacol.*, **30**, 156 (2023).
14. M.T.H. Albuquerque, M.M.C. Santos, A.S.J. Cavaleiro and M.S.A. Silva, *Curr. Org. Chem.*, **18**, 2750 (2014); https://doi.org/10.2174/1385272819666141013224253
15. F.F. Leite, N.F. de Sousa, B.H.M. de Oliveira, G.D. Duarte, M.D.L. Ferreira, M.T. Scotti, J.M.B. Filho, L.C. Rodrigues, R.O. de Moura, F.J.B. Mendonça-Junior and L. Scotti, *Molecules*, **28**, 4009 (2023); https://doi.org/10.3390/molecules28104009
16. A. Shaik, R. Bhandare, K. Palleapati, S. Nissankararao, V. Kancharlapalli and S. Shaik, *Molecules*, **25**, 1047 (2020); https://doi.org/10.3390/molecules25051047
17. A. Usta, E. Öztürk and F.S. Beris, *Nat. Prod. Res.*, **28**, 483 (2014); https://doi.org/10.1080/14786419.2013.879472
18. V. Desai, S. Desai, S.N. Gaonkar, U. Palyekar, S.D. Joshi and S.K. Dixit, *Bioorg. Med. Chem. Lett.*, **27**, 2174 (2017); https://doi.org/10.1016/j.bmcl.2017.03.059
19. B.S. Kitawat, M. Singh and R. Kathalupant Kale, *New J. Chem.*, **37**, 2541 (2013); https://doi.org/10.1039/c3nj00308f
20. E. Królicka, K. Kiec-Kononowicz and D. Lazewska, *Pharmaceuticals*, **15**, 847 (2022); https://doi.org/10.3390/ph15070847

21. C. Minders, J. Petzer, A. Petzer and A. Lourens, *Bioorg. Med. Chem. Lett.*, **25**, 5270 (2015); https://doi.org/10.1016/j.bmcl.2015.09.049
22. C. Zhuang, W. Zhang, C. Sheng, W. Zhang, C. Xing and Z. Miao, *Chem. Rev.*, **117**, 7762 (2017); https://doi.org/10.1021/acs.chemrev.7b00020
23. K. Mezgebe, Y. Melaku and E. Mulugeta, *ACS Omega*, **8**, 19194 (2023); https://doi.org/10.1021/acsomega.3c01035
24. M.G.S. De Padua, M.J. De Souza, C.M.M. Sales, G.L. De Vasconcelos, L.E. Dall'Oglio, T.M. Faraggi, M.O. Sampaio and C.C.L. Vieira, *Chem. Biodivers.*, **18**, e2100226 (2021); https://doi.org/10.1002/cbdv.202100226
25. H. Chen, G. Noirbent, S. Liu, D. Brunel, B. Graff, D. Gigmes, Y. Zhang, K. Sun, F. Morlet-Savary, P. Xiao, F. Dumur and J. Lalevée, *Mater. Chem. Front.*, **5**, 901 (2021); https://doi.org/10.1039/D0QM00755B
26. R.A. Friesner, R.B. Murphy, M.P. Repasky, L.L. Frye, J.R. Greenwood, T.A. Halgren, P.C. Sanschagrin and D.T. Mainz, *J. Med. Chem.*, **49**, 6177 (2006); https://doi.org/10.1021/jm051256o
27. D. Eisenberg, R. Luthy and J.U. Bowie, *Methods Enzymol.*, **277**, 396 (1997); https://doi.org/10.1016/S0076-6879(97)77022-8
28. C. Colovos and T.O. Yeates, *Protein Sci.*, **2**, 1511 (1993); https://doi.org/10.1002/pro.5560020916
29. S. Analysis and V. Server, 2011. Available from: http://nihserver.mbi.ucla.edu/SAVES/.
30. S.C. Lovell, I.W. Davis, W.B. Arendall 3rd, P.I. de Bakker, J.M. Word, M.G. Prisant, J.S. Richardson and D.C. Richardson, *Proteins*, **50**, 437 (2003); https://doi.org/10.1002/prot.10286
31. Cambridge Soft Corporation, a subsidiary of PerkinElmer, Inc. (2014). Chem DrawUltra version 8.0.3 for Windows. Available from: www.cambridgesoft.com.
32. https://sourceforge.net/projects/openbabel/files/openbabel/2.4.0/. License: GNU GPL v2.
33. N.M. O'Boyle, M. Banck, C.A. James, C. Morley, T. Vandermeersch and G.R. Hutchison, *J. Cheminform.*, **3**, 33 (2011); https://doi.org/10.1186/1758-2946-3-33
34. E. Harder, W. Damm, J. Maple, C. Wu, M. Reboul, J.Y. Xiang, L. Wang, D. Lupyan, M.K. Dahlgren, J.L. Knight, J.W. Kaus, D.S. Cerutti, G. Krilov, W.L. Jorgensen, R. Abel and R.A. Friesner, *J. Chem. Theory Comput.*, **12**, 281 (2016); https://doi.org/10.1021/acs.jctc.5b00864
35. S.G. Franzblau, R.S. Witzig, J.C. McLaughlin, P. Torres, G. Madico, A. Hernandez, M.T. Degnan, M.B. Cook, V.K. Quenzer, R.M. Ferguson and R.H. Gilman, *J. Clin. Microbiol.*, **36**, 362 (1998); https://doi.org/10.1128/JCM.36.2.362-366.1998
36. B. Aneja, M. Azam, S. Alam, A. Perwez, R. Maguire, U. Yadava, K. Kavanagh, C.G. Daniliuc, M.M.A. Rizvi, Q.M.R. Haq and M. Abid, *ACS Omega*, **3**, 6912 (2018); https://doi.org/10.1021/acsomega.8b00582
37. CLSI, M100 Performance Standards for Antimicrobial Susceptibility Testing. 29th ed. CLSI; Wayne, PA, USA: 2019.